Real-world Objects Scaffold Visual Working Memory for Features: Increased Neural Engagement When Colors Are Remembered as Part of Meaningful Objects

Yong Hoon Chung[1], Timothy F. Brady[2], and Viola S. Störmer[1]

Abstract

■ Visual working memory is a core cognitive function that allows active storage of task-relevant visual information. Contrary to the common assumption that the capacity of this system is fixed with respect to a single feature dimension, recent research has shown that working memory performance for a simple visual feature—color—is improved when this feature is encoded as part of a real-world object relative to an unrecognizable scrambled object. Using EEG (n = 24), we here demonstrate that this performance benefit is supported by increased neural engagement during the retention period, as indexed by enlarged contralateral delay activity during maintenance. Furthermore, the pattern of neural activity across parietal-occipital electrodes was more stable across time, suggesting that real-world objects may support more robust memory representations. Finally, we report a novel fronto-central ERP that distinguishes between real-world objects and scrambled objects during encoding and maintenance processes. Overall, our results demonstrate that active visual working memory capacity for simple features is not fixed but can expand depending on what context these features are encoded in. ■

INTRODUCTION

Visual working memory supports the active storage of task-relevant visual information (Bays et al., 2024; Baddeley & Hitch, 1974). Its capacity is typically assessed by presenting multiple items composed of simple visual features (color, orientation) and abstract shapes (circles, polygons) for brief durations, as these conditions and stimuli are believed to best isolate visual working memory capacity separate from rehearsal, chunking, and passive memory systems (Cowan, 2001). One major conclusion from studies using such stimuli is that the capacity to maintain visual information is strictly limited, often quantified in terms of the number of objects (Awh & Vogel, 2025; Adam et al., 2017; Cowan, 2001; Luck & Vogel, 1997) or in terms of a fixed resource pool within each simple visual feature dimension that is distributed among the encoded items (e.g., Bays, 2014; Bays et al., 2009).

However, more recent research has demonstrated that working memory capacity is not fixed but depends on the kind of information stored: Familiar and meaningful stimuli, such as real-world objects, result in increased neural maintenance activity and better behavioral performance compared with abstract and nonmeaningful shapes (Thibeault et al., 2024; Torres et al., 2025; Asp et al., 2021; Brady, Störmer, & Alvarez, 2016). One explanation for this benefit is that these stimuli allow participants to extract more relevant visual and semantic features and can thus recruit additional neural populations and cognitive resources to support maintenance (see Chung, Brady, & Störmer, 2024b, for a review), similar to how maintaining both color and orientation allows the storage of more total information than color alone (Shin & Ma, 2017; Luck & Vogel, 2013).

Recent studies significantly expanded on these findings, demonstrating that working memory performance can be improved within a single feature dimension—color—when this feature is encoded in a meaningful context (Chung, Brady, & Störmer, 2024a; Chung, Brady, & Störmer, 2023). Specifically, in a series of behavioral experiments, participants showed better color memory performance when these colors were presented as parts of real-world objects (e.g., a blue backpack) at encoding compared with unrecognizable scrambled shapes, even though the color–object associations were randomly chosen on every trial, and object identity itself was task irrelevant. These findings provide a challenge to fixed-capacity models of working memory, which assume that how much information can be maintained is strictly limited within a single feature dimension. They also move beyond the real-world memory advantage previously shown for entire object identities (i.e., remembering a chair better than a colored circle), demonstrating that memory performance even for simple low-level features that are parts of objects can be modulated by encoding context (i.e., a color superimposed on a chair is better remembered than the same color on a scrambled object).

What explains this improvement for feature working memory specifically? The observed behavioral effects could be supported by increases in active working memory usage; they could be due to more efficient coding of real-world objects compared with abstract stimuli,

[1]Dartmouth College, [2]University of California San Diego

potentially freeing up resources to better remember the colors; or the performance benefits could be merely due to differences at retrieval, with no changes during active maintenance. To disambiguate between these possibilities, we here examine both the amplitude and stability of neural activity during the maintenance period of a working memory task. Persistent neural activity during maintenance is the hallmark of working memory functioning and not present when participants rely on other nonactive forms of storage for retaining information (Buschman et al., 2011; Vogel & Machizawa, 2004). One particularly strong marker of active working memory is the contralateral delay activity (CDA), a sustained negativity of the ERP indexing how much visual information is actively maintained (Vogel & Machizawa, 2004; for a review, see Luria, Balaban, Awh, & Vogel, 2016). The amplitude of the CDA tracks active storage, increasing as more information is actively retained (Salahub et al., 2019; Carlisle et al., 2011; Vogel, McCollough, & Machizawa, 2005); it is more sensitive to visual than verbal load (Predovan et al., 2008); it can selectively isolate memory for task-relevant features (Woodman & Vogel, 2008); and it remains robust to low-level visual changes such as contrast (Ikkai et al., 2010). Moreover, the lateralized nature of the CDA is believed to effectively control for bilateral ERP differences that may reflect differences in overall perceptual processing, making it suitable for examining how different stimulus types influence active visual working memory storage for simple features. Thus, we capitalize on this well-established neural marker to examine whether better color memory for real-world objects reflects increased, decreased, or unchanged active maintenance. In addition to the CDA, we examined the stability of the pattern of neural activity over the delay, as an index of the robustness of the memory representation across time. Overall, our results suggest that improved color memory is supported by increased neural engagement during encoding and delay.

EXPERIMENT 1: ASSESSING COLOR WORKING MEMORY PERFORMANCE

In Experiment 1, we assessed the behavioral performance of color working memory for intact objects compared with scrambled objects. Previous studies showed that color working memory is significantly improved when the colors are remembered as parts of meaningful real-world objects (Chung et al., 2023). Here, we aimed to replicate these behavioral effects.

Methods

The experiment was approved by the internal review boards at University of California San Diego and Dartmouth College. The sample size, hypotheses, analysis plans, and exclusion criteria for Experiment 1 were preregistered (https://aspredicted.org/fwhh-h82k.pdf).

Participants

All participants gave informed consent before participating in this experiment. The sample size of the EEG investigation was a priori determined to be 24 participants (see the Methods section below). To achieve greater power for the behavioral effect replication, we doubled the planned sample size in Experiment 1 to be 48 participants. In total, 58 participants were recruited from the University of California San Diego online recruitment platform. Participants' ages ranged from 18 to 35 years. Following the preregistered exclusion criteria similar to prior works (e.g., Chung et al., 2023), we excluded participants' data if their overall behavioral performance across conditions was lower than $d' < 0.5$ or if more than 10% of their trials were excluded. Individual trials were excluded if the RT was shorter than 200 msec or longer than 5000 msec. This resulted in 10 participants' data being excluded, resulting in data from 48 participants for the final analysis.

Stimuli

For the intact object condition, a subsample of 405 real-world object images was drawn from the database of Brady, Konkle, Gill, Oliva, and Alvarez (2013). These objects are generally color-neutral in everyday life and can be assigned any single arbitrary color. Following Chung and colleagues (2023), we rotated the stimuli in hue space along a CIE L*a*b* color wheel, so that any object could occur in any color along the wheel. For the scrambled object condition, these object images were then morphed using the diffeomorphic scrambling technique (Stojanoski & Cusack, 2014), similar to previous work (e.g., Chung, Tam, Wyble, & Störmer, 2025; Chung et al., 2023, 2024a; Thibeault et al., 2024; Brady & Störmer, 2022). This transformation technique is particularly useful as it can make object images unrecognizable while maintaining their basic perceptual features and visual complexity. None of the object stimuli were repeated throughout the experiment. The exact sizes of the stimuli varied slightly, but they were placed in a white area that extended 135 pixels in height and 135 pixels in width. The colors of stimuli on each trial were randomly selected along the 360° color wheel with the constraint that they had to be at least 30° apart from each other, including the foil stimulus at test. This was done so that all colors presented in each trial were discernibly different, and there were no overlapping colors causing interference or confusion at test.

Experimental Procedure

This was an online experiment where participants completed the study with their own devices. On each trial, participants were presented with an array of three stimuli simultaneously evenly distributed around the central fixation cross for 800 msec. On half of the trials, colored real-world objects were presented, and on the remaining half of trials, colored scrambled objects were presented. Afterward, an 800-msec delay period followed, displaying a blank

screen with the central fixation cross. At test, one stimulus from the encoding period appeared in two different colors around the center of the screen, and participants were asked to indicate which of the two colors they had encoded initially by clicking the corresponding item. Following previous work (Chung et al., 2023), one of the stimulus choices appeared in the color that matched the encoded color (target) and the other stimulus appeared in a color 180° away from the target color on the color wheel (foil). The foil colors were also at least 30° away from the other stimulus colors in the encoding array, ensuring no overlap in colors among stimuli on each trial. After the two-alternative forced choice (2-AFC) task, participants received feedback in the form of a sound. Note that throughout the experiment, participants were never asked to recall the identities of the stimuli and were only asked about their colors. Thus, the experiment could be done without any regard for the identity of the stimuli. Participants completed 270 trials total (135 trials each condition, randomly intermixed). Before the experiment, participants viewed a 10-sec video of the task, familiarizing themselves with the task design. See Figure 1A for an illustration of the trial structure.

Statistical Analysis

Performance on the color memory task was quantified as d' for a 2-AFC task (([zhits] − [zfalse alarms])/√2) for each participant and condition separately (intact object condition vs. scrambled object condition). The d' values were then statistically compared using a paired t test. In addition, following previous work (Asp et al., 2021), we also fit a linear mixed effects model with the participant as a random factor for more sensitive statistical tests (see Supplemental Materials).

Results

We found a significant increase in color working memory performance for the intact objects (mean d' = 1.15) compared with scrambled objects (mean d' = 1.02): $t(47)$ = 3.47, p = .001, Cohen's d_z = 0.34 (see Figure 1B). This shows a reliable replication of the previously found meaningfulness benefit in feature working memory (Chung et al., 2023, 2024a).

EXPERIMENT 2: ASSESSING ACTIVE WORKING MEMORY ENGAGEMENT WITH EEG

Experiment 1 showed improved color working memory performance for intact real-world objects compared with scrambled objects. In Experiment 2, we used EEG to uncover the active working memory engagement during the encoding and maintenance periods of the working memory task.

Methods

The experiment was approved by the Committee for the Protection of Human Subjects at Dartmouth College.

Participants

All participants gave written informed consent before participating in this experiment. To obtain our goal of 24 usable EEG participants, 29 participants were recruited from Dartmouth College using their online recruitment platform. Participants' ages ranged from 18 to 35 years, and all participants had normal or corrected-to-normal vision. Before the experiment, participants were given

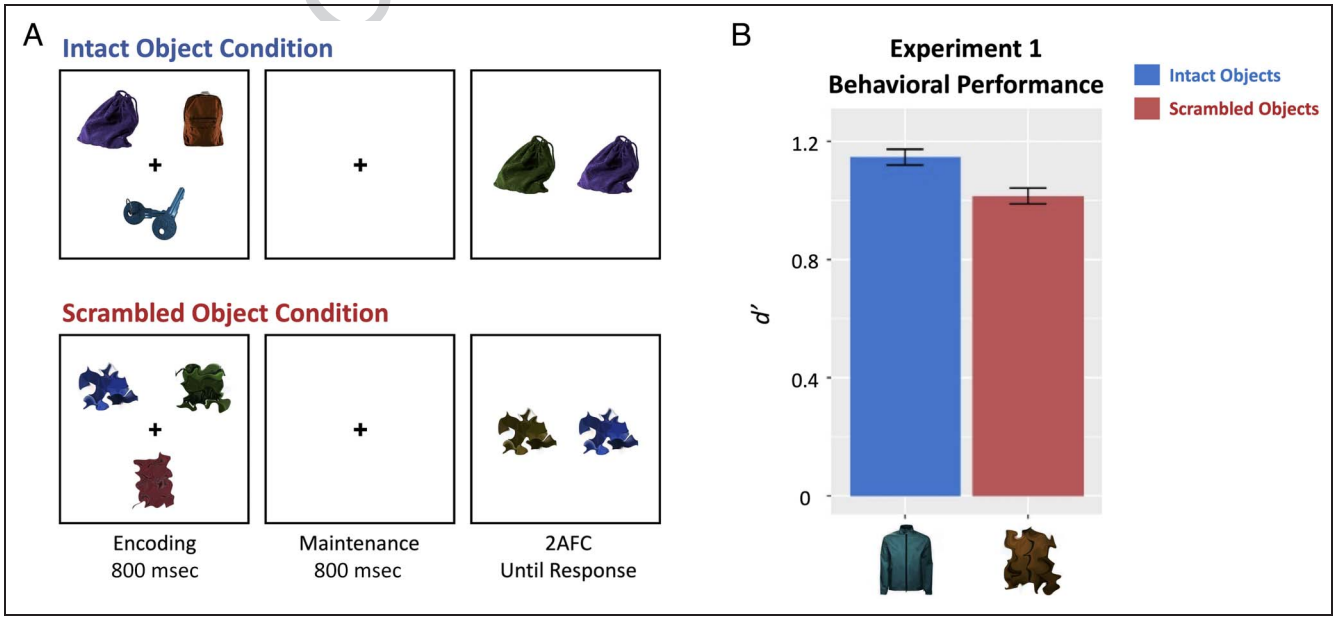

Figure 1. (A) Trial structure of Experiment 1. All stimulus sizes and distances are for illustration purposes only. (B) Behavioral performance results of Experiment 1 (n = 48).

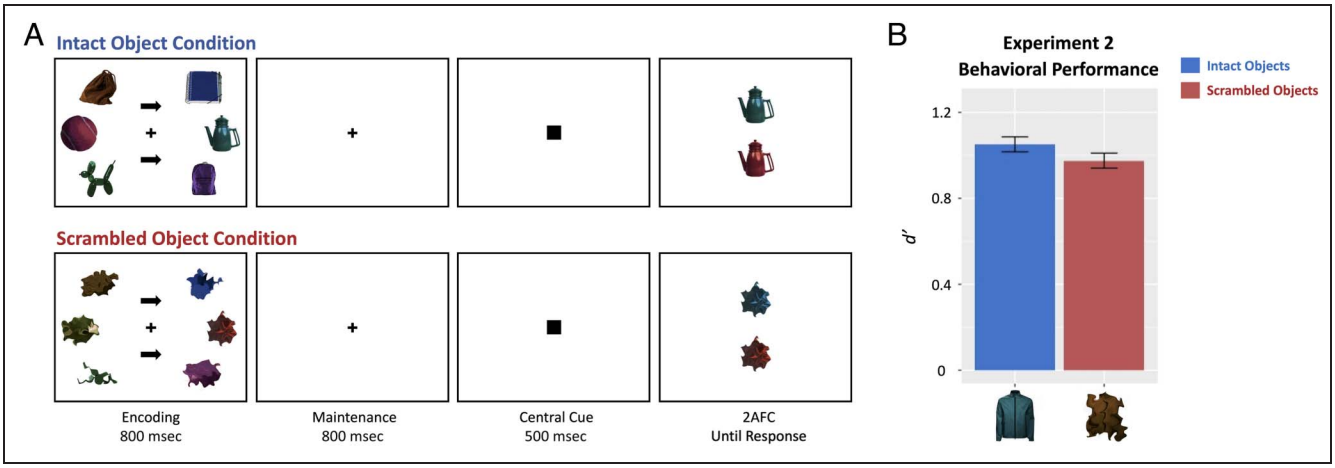

Figure 2. (A) Trial structure of Experiment 2. All stimulus sizes and distances are for illustration purposes only. (B) Behavioral performance results of Experiment 2 based on the 24 participants used in the main EEG analysis.

the Ishihara color blindness test (Clark, 1924). Similar to Experiment 1, participants' behavioral and EEG data were excluded if their overall behavioral performance was lower than $d' < 0.5$. Their EEG data were excluded if more than 40% of trials were excluded due to EEG artifact rejection. No participant was excluded due to behavioral performance. Five participants were excluded from the EEG analysis due to artifact rejection, totaling our target of 24 participants. On average, about 17.7% of trials were rejected due to EEG artifacts across the remaining participants. The final sample size of 24 for the EEG analysis was determined following protocols of previous studies investigating CDA measures of meaningful stimuli (e.g., 19 participants in Asp et al., 2021; 18 participants in Brady et al., 2016; 22 participants in Thibeault et al., 2024). In addition, a post hoc power analysis based on the observed effect size of CDA (Cohen's $d_z = 0.59$), alpha level of .05, and desired power of 0.80 indicated that a minimum of 24 participants would be required to detect this effect.

Stimuli

Stimuli used in Experiment 2 were similar to Experiment 1, except all 540 real-world object images were sampled from Brady and colleagues (2013). On a given trial, three colored objects appeared on each side of the screen. Two of the stimuli were centered 4.1° of visual angle away from the fixation along the horizontal meridian and ±3.5° of visual angle along the vertical meridian, whereas the other one was centered 9.7° away from fixation along the horizontal meridian, centered on the vertical meridian (see Figure 2A for an illustration). The exact stimulus size varied slightly across objects, but they were all centrally placed in a white area that extended 5.2° in height and 5.2° in width in visual angle for the two of objects at the top and bottom locations, and 5.7° in height and 5.7° in width for the object presented along the horizontal meridian that was more distant from fixation. Similar to Experiment 1, the colors of objects on each side of the screen were randomly selected along the 360° color wheel with the constraint that they had to be at least 30° apart from each other. Due to the limited number of objects sampled, some objects repeated throughout the experiments. However, none of the objects repeated more than once, and this was the same across the two conditions.

Experimental Procedure

Similar to Experiment 1, participants were instructed to remember the colors of three stimuli over a brief delay period. Throughout each trial, a small black fixation cross was presented in the center of a white screen and participants were instructed to maintain fixation. We used a lateralized memory display to allow the measurement of the lateralized CDA component. Thus, the memory encoding display consisted of three stimuli presented on each of the left and right sides of the screen along with two black arrow cues at the center of the screen (one above and one below the fixation cross) pointing toward the to-be-remembered side (left or right). On half of the trials, colored real-world objects were presented, and on the remaining half of trials, colored scrambled objects were presented. Participants were instructed to remember the colors of the stimuli on the side that the arrows pointed to while maintaining their gaze on the central fixation cross. After an 800-msec encoding period, an 800-msec delay period followed, displaying a blank screen with just the central fixation cross, followed by a probe (a small black square, 0.9° height and width; 500 msec) that appeared at the center of the screen, prompting participants of the beginning of the response period. Subsequently, participants performed the 2-AFC task where one stimulus from the to-be-remembered side appeared in two different colors around the center of the screen (slightly shifted along the vertical meridian), and participants were asked to indicate which of the two colors they had encoded initially by pressing up and down arrow keys on the keyboard corresponding to the relative position of the items on the

screen (top vs. bottom). The stimuli for the 2-AFC task were chosen the same way as in Experiment 1. After the response, participants received feedback in the form of a fixation cross color change (green correct, red incorrect) after which the screen turned fully white. After each trial, participants could start the next trial with a button press. The next trial then began after an intertrial interval (ITI) of 800 msec (first 19 participants) or randomly jittered 600–1000 msec (last five participants). Participants completed 432 trials in total (216 trials each condition, randomly intermixed) and also went through a practice block of 10 trials before the main experiment. See Figure 2A for an illustration of the trial structure.

Electrophysiological Recording

EEG was recorded continuously from 32 Ag/AgCl electrodes (arranged in the 10–20 system) mounted in an elastic cap and amplified by an ActiCHamp amplifier (BrainProducts). The HEOG was recorded from two additional electrodes positioned on the external ocular canthi, which were grounded with another electrode placed on the neck of the participant. All scalp electrodes were referenced to the right mastoid online and were digitized at 500 Hz. EEG data were filtered with a bandpass of 0.01–112.5 Hz online.

Statistical Analysis

Behavioral data analysis. The behavioral analysis was identical to Experiment 1.

EEG analysis. All EEG data analyses were performed using EEGLAB (Delorme & Makeig, 2004) and ERPLAB (Lopez-Calderon & Luck, 2014) toolboxes and custom-written scripts. Data were epoched into trials aligned to the onset of the encoding display. Artifacts were detected using an automated pipeline, and artifact rejection was performed from 200 msec before the onset of memory stimuli to 1600 msec afterward (the end of the delay period). Trials with eye blinks (peak-to-peak at channel FP1, threshold at 150 μV), excessive eye movements (step function at HEOG, threshold at 17 μV that corresponds to ~1° of saccade; cf. Luck, 2014; Hillyard & Galambos, 1970), and large noise (peak-to-peak all channels, threshold at 300 μV) were excluded from the analysis. The average rejection rate of participants included in the final analysis was 17.7%. Artifact-free data were rereferenced to the average of the left and right mastoids, digitally low-pass filtered at 30 Hz (Butterworth filter, 12 dB/octave roll-off), and baseline corrected to the 200-msec prestimulus interval.

Parietal-occipital lateralized ERPs. We examined lateralized activity over posterior electrode sites both during the encoding (400–800 msec) and delay (1200–1600 msec) periods. Our main interest was to assess whether remembered colors of real-world objects versus scrambled objects result in a difference in the delay period (the CDA), as this marks the active maintenance of visual representations (Adam et al., 2018; Unsworth et al., 2015; McCollough et al., 2007; Vogel & Machizawa, 2004). However, based on recent findings indicating that lateralized differences may emerge during the encoding period when using relatively long encoding times and meaningful stimuli (cf. Thibeault et al., 2024; Asp et al., 2021), we included both time intervals in our main analyses. EEG epochs were averaged separately for each object condition (intact vs. scrambled) and hemifield (remember left vs. right) and were then collapsed across to-be-remembered visual hemifield (left/right) and hemisphere of recording (left/right) to obtain waveforms recorded over the hemisphere contralateral and ipsilateral with respect to the to-be-remembered side. To quantify the activity that was related to the encoding and memorization of the cued items in particular, the ipsilateral waveform was subtracted from the contralateral waveform. Thus, this difference wave reflects the increase in neural activity that is specific to the to-be-remembered items, removing purely sensory-related activity. The mean amplitude for each participant was calculated by averaging activity across four posterior-occipital electrode pairs (PO3/PO4, PO7/PO8, P7/P8, and O1/O2; Asp et al., 2021) from 400 to 800 msec post stimulus onset for the encoding period and 400 msec to 800 msec after the stimuli offset (1200–1600 msec post encoding display onset). Electrode sites and CDA time windows were chosen a priori based on previous studies (see Roy & Faubert, 2023, for a review); the encoding period time window was chosen to avoid early visually evoked potentials (i.e., P1/N1) and match the duration of the CDA analysis. For each time window, mean amplitudes were compared across conditions (intact vs. scrambled) using paired t tests.

We also examined differences in the topographies across the two conditions during both encoding and delay time periods. Scalp topographies of the lateralized encoding and retention periods are plotted in Figure 3D as the contralateral-minus-ipsilateral difference waveform, projected on the right side of the scalp. To statistically compare these topographies, we first normalized the difference waveform by dividing the amplitude from each electrode site by the square root of the sum of the squared voltages across all electrodes within each condition (McCarthy & Wood, 1985) to ensure differences in overall amplitudes would not drive the differences in results. Then, we ran a 2 × 2 ANOVA with 13 lateralized Electrode Pairs and two Conditions (intact vs. scrambled objects) as within-subject factors.

Cross-temporal pattern similarity. To evaluate the neural stability of the memory representations for each condition, we adopted a novel analysis method (inspired by a different multivariate decoding approach by Spaak et al., 2017; see also Liu et al., 2020) comparing the pattern

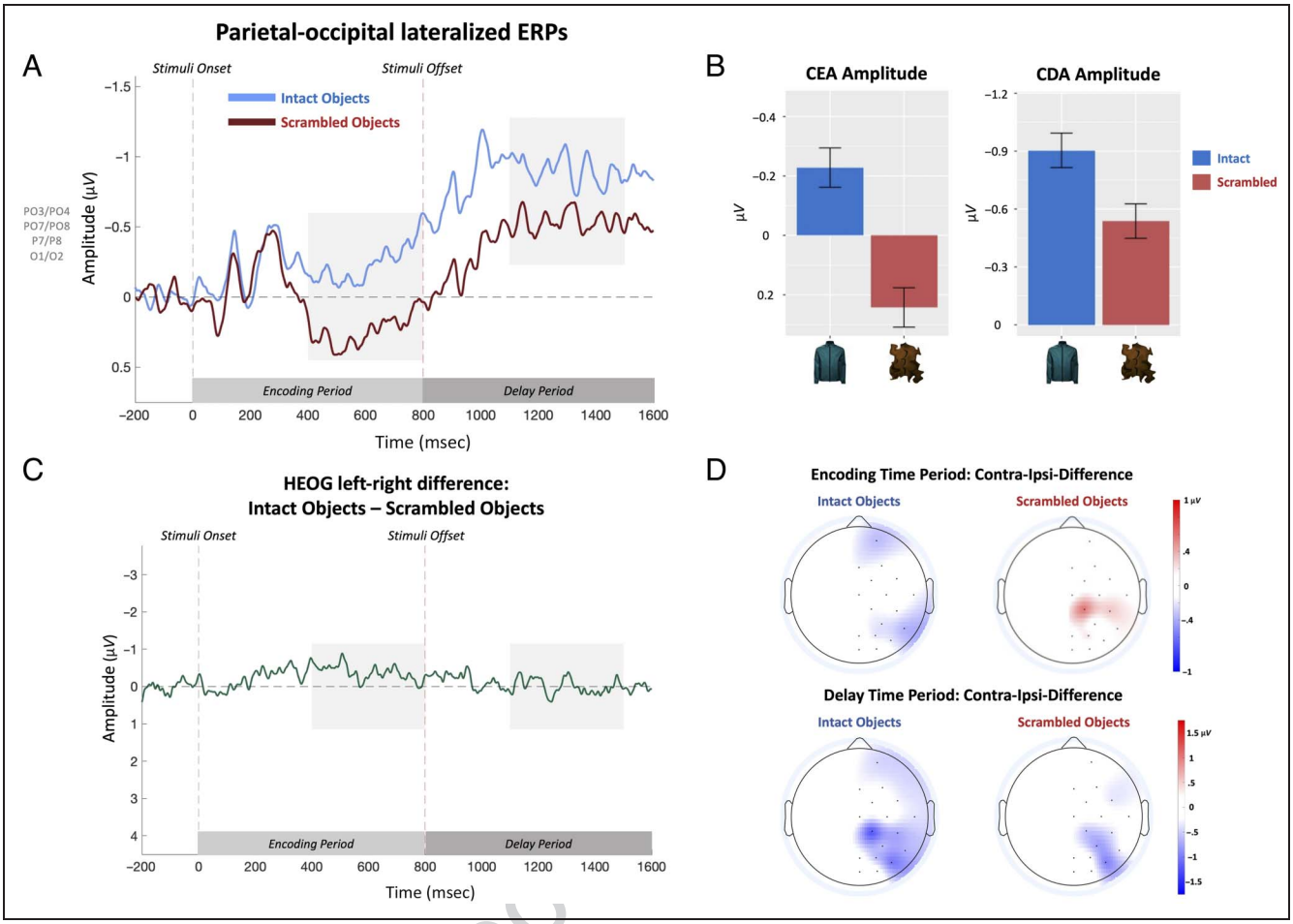

Figure 3. (A) Contralateral-minus-ipsilateral waveforms averaged over parietal-occipital electrodes separately for intact (light blue) and scrambled (dark red) object conditions. Highlighted areas depict the time windows for the ERP analyses for the CEA and CDA. (B) Mean CEA and CDA amplitudes separately for each condition. Error bars reflect within-subject standard errors of the mean. (C) HEOG subtraction waveforms. Highlighted areas are the time windows for CEA and CDA analyses. (D) Spatial topographies of the contralateral-minus-ipsilateral waveforms during the encoding and delay time periods. Mean difference is projected on the right side of the scalp. Note that the scale differs between encoding (top) and delay (bottom) time periods.

similarity of the lateralized difference waveforms across time. Our main goal was to evaluate whether the patterns of electrical activity across encoding and maintenance periods would differ in terms of their stability across the two conditions. Such multivariate stability measures would not be reflected in univariate amplitude changes assessed via the CDA component. To examine the temporal stability, separately for each condition, we computed the cosine similarities of the activity pattern of these ERP waveforms over time, smoothed over 10 msec. We separated this similarity analysis into two sets of electrodes, one using a set of parietal-occipital electrodes (P7/P8, P3/P4, PO3/PO4, PO7/PO8, O1/O2) and one using a set of fronto-central electrode (FP1/FP2, F3/F4, FC1/FC2, FC5/FC6, C3/C4); given that this was a visual working memory task, we expected the posterior set of electrodes to be more sensitive to the condition differences. Figure 4A depicts the resulting cross-temporal analysis matrices that show the neural activity similarity time by time across the entire trial period, separately for posterior (top) and anterior (bottom) scalp sites. Higher cross-temporal similarity may reflect more stable representations. Across all conditions, we observed an increase in similarity across time. The critical question was whether this increase in neural stability arose at different points in time for the intact versus scrambled object condition. To test this, we collapsed the cross-temporal similarity matrices by averaging the similarity values between a given time point and the average of all later time points (i.e., mean cosine similarities of $t1$ vs. $t2$-tn; $t2$ vs. $t3$-tn, etc.). We then statistically compared the time courses of the average similarity values across conditions using a cluster-based permutation t test. At each time bin (10 msec), we performed a paired t test comparing the similarity values for the real and scrambled conditions across participants. Contiguous time bins with uncorrected p values below .05 were grouped into clusters. For each cluster, we summed the t values to create a cluster-level test statistic. To assess significance, we generated a null distribution by randomly permuting the time bin labels within each participant 1000 times and recomputing the t tests and cluster-level statistics for each permutation. The

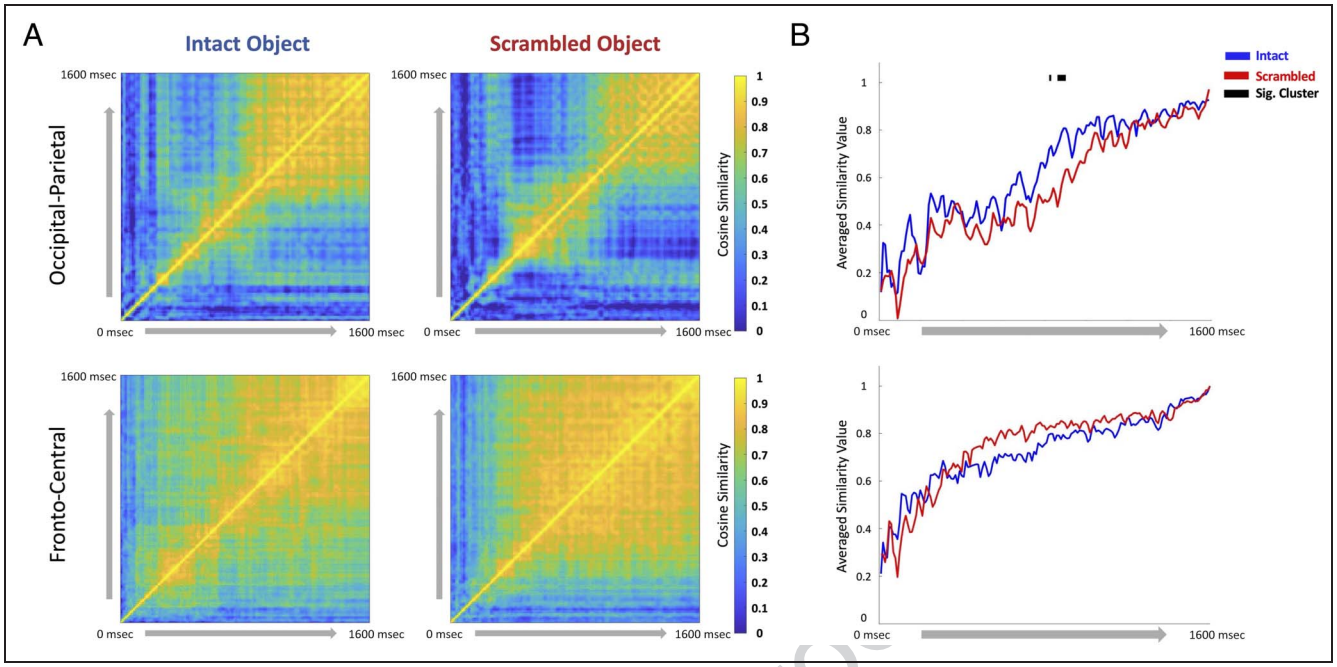

Figure 4. (A) Cross-temporal stability matrices depicting cosine similarities of lateralized ERP waveform patterns across time. Matrices on top are parietal-occipital electrode sites whereas the bottom ones are fronto-central electrode sites. (B) Cosine similarity values between each time window and all later time windows were averaged to compare the time course of stability across the two conditions. Generally, ERP patterns became more stabilized over time, indicated by upward trends of the averaged similarity values. For parietal-occipital sites, the neural activity pattern for intact objects became stable earlier compared with scrambled objects, as indicated by the significant difference around 800–900 msec.

p value for each observed cluster was computed as the proportion of permuted cluster-level statistics that exceeded the observed cluster sum. This procedure controls for multiple comparisons while preserving the temporal structure of the data.

We note that this was an exploratory analysis aimed at assessing the temporal evolution of the lateralized ERP signal, which provides complementary insights to the traditional CDA analysis. Whereas the CDA typically reflects the overall amplitude of neural delay activity within a fixed time window, this approach examines how stable or changing the neural patterns are over time. Conceptually, more versus less consistent activity patterns might reflect stability or shifts in the representational state of working memory, and these changes may not directly be tied to differences in overall storage load (e.g., higher CDA amplitudes do not necessarily indicate more stable patterns across time).

Bilateral fronto-central ERPs. As an exploratory analysis, we also compared nonlateralized neural activity between the two experimental conditions at fronto-central electrode sites (FC1, FC2, CP1, CP2, Cz) during both the encoding and delay periods using the same time windows as for the lateralized ERPs (400–800 msec and 1200–1600 msec post stimulus onset). The mean ERP amplitudes between the two conditions were compared using a paired *t* test. Note that such global differences in bilateral activity is controlled for in the main CDA analysis as nonlateralized activity is subtracted out.

Results

Behavioral Results

We first analyzed the behavioral data including all the participants who met the behavioral inclusion criteria (all 29 participants). This revealed the expected increase in color working memory performance for the intact objects (mean $d' = 1.09$) compared with the scrambled objects (mean $d' = 0.98$): $t(28) = 2.25$, $p = .03$, Cohen's $d_z = 0.43$, replicating Experiment 1 and other previous studies (Chung et al., 2023, 2024a). When only including the 24 participants that were retained for the EEG analysis after artifact rejection, this effect remained numerically present, although it was statistically nonsignificant (mean $d' = 1.05$ for intact objects vs. 0.98 for scrambled, $t(23) = 1.54$, $p = .14$, Cohen's $d_z = 0.32$; see Figure 2B).

We believe that the nonsignificant behavioral result in Experiment 2 with 24 participants likely reflects a Type 2 error, as (1) the effect size in Experiment 2 ($d_z = 0.32$) was comparable with those observed in our larger-sample Experiment 1 ($d_z = 0.34$) and in prior studies (e.g., Chung et al., 2023, Set Size 3 in Experiment 3 $d_z = 0.48$); (2) the effect is statistically reliable when including all 29 tested participants, $t(28) = 2.25$, $p = .03$, $d_z = 0.43$; and (3) a more sensitive generalized linear mixed-effects model including subject as a random factor (following Asp

et al., 2021) also revealed a significant effect of condition ($\beta = -0.09$, $z = -1.96$, $p = .049$; see Supplemental Materials).

Contralateral Encoding Activity (CEA)

All EEG analyses focused on the 24 participants who met the EEG inclusion criteria. During the encoding period (400–800 msec), colors superimposed on intact objects elicited a larger contralateral versus ipsilateral negativity (mean amplitude = −0.23 μV) relative to colors superimposed on scrambled stimuli (mean amplitude = 0.24 μV): $t(23) = 5.03$, $p < .001$, Cohen's $d_z = 0.89$ (see Figure 3A and B). This pattern was present when including all 29 participants' data (see Supplemental Materials).

Statistical analysis of the spatial topography during encoding resulted in a significant interaction between the Memory Conditions and Electrode Sites, $F(12, 276) = 2.42$, $p = .005$, $\eta_p^2 = .095$, indicating a shift in the pattern of activity across conditions. There was also a significant main effect of Condition, $F(1, 23) = 5.18$, $p = .03$, $\eta_p^2 = .18$, but no main effect of Electrode Locations, $F(12, 276) = 1.42$, $p = .15$, $\eta_p^2 = .06$. Visual inspection suggests that the intact object condition showed a more lateralized parietal-occipital focus, whereas the scrambled object condition showed a more central-parietal focus of activity (see Figure 3D).

CDA

During the retention period, mean CDA amplitude (1200–1600 msec) was significantly more negative (mean amplitude = −0.90 μV) for the intact object condition than the scrambled object condition (mean amplitude = −0.54 μV): $t(23) = 2.90$, $p = .008$, Cohen's $d_z = 0.59$ (see Figure 3A and B), indicating that active maintenance activity was increased for colors superimposed on real objects at encoding. This pattern was present when including all 29 participants' data (see Supplemental Materials).

The topographical analysis revealed a significant interaction between the Memory Conditions and Electrode Sites, $F(12, 276) = 2.003$, $p = .02$, $\eta_p^2 = .08$, indicating a reliable difference in the spatial distribution of activity, similar as during the encoding period. There was no main effect of Condition, $F(1, 23) = 1.23$, $p = .28$, $\eta_p^2 = .05$), but there was a significant main effect of Electrode Location, $F(12, 276) = 3.89$, $p < .001$, $\eta_p^2 = .15$. Visual inspection of the spatial topographies suggests that the activity pattern was more spread out toward parietal-central and temporal electrode sites for the intact object condition compared with the scrambled condition, in addition to increasing in amplitude (see Figure 3D).

Cross-Temporal Pattern Similarity

The cross-temporal matrices for intact versus scrambled object conditions, separately for parietal-occipital and fronto-central electrode channels, are shown in Figure 4A. Overall, as time evolves, neural stability increases across both conditions. Visual examination of these cross-temporal matrices suggests that the neural pattern became stable earlier for intact versus scrambled objects, especially over parietal-occipital electrode sites. Our statistical analysis examining the time course of neural stability supported this, resulting in a cluster of significant differences in stability between the two conditions around 800–900 msec for the occipital-parietal electrode sites (see Figure 4B, top). Thus, it appears that differences in neural stability arose during late encoding to early delay time period, although the precise timing of significant clusters should be interpreted with caution given the known limitations of cluster-based permutation tests (Sassenhagen & Draschkow, 2019). In contrast, no reliable differences in neural stability between the two conditions were found for the fronto-central electrode sites (Figure 4B, bottom).

HEOG

To ensure that the observed lateralized effects (e.g., CEA, CDA) were not attributable to systematic eye movement differences between conditions, we analyzed the HEOG waveforms for each cued side (left/right) across the object conditions (intact/scramble) during both the CEA and CDA time windows. Specifically, we subtracted the HEOG activity of the remember-right condition from the activity of the remember-left condition, separately for each object condition; then, we subtracted the scrambled object condition from the intact object condition. These subtracted HEOG waveforms were then tested against zero using single-sample t tests. The results indicated that the subtracted HEOG waveforms did not significantly deviate from zero in either time window: CEA: $t(23) = 1.07$, $p = .29$; CDA: $t(23) = 0.02$, $p = .98$ (see Figure 3C). This suggests that the observed differences in CEA and CDA across the conditions were not driven by differences in systemic eye movements.

Bilateral Fronto-central Negativity during Encoding and Delay Period

We observed a robust nonlateralized ERP difference over fronto-central electrode sites across the intact and scrambled object conditions. Specifically, the intact object condition elicited a large negative slow-wave relative to the scrambled object condition during the encoding period, $t(23) = 9.25$, $p < .001$, Cohen's $d_z = 0.69$, which sustained throughout the delay period, $t(23) = 4.06$, $p < .001$, Cohen's $d_z = 0.32$ (see Figure 5A, B, and C). This suggests that the activity over fronto-central electrode sites tracks the meaningfulness of items at encoding and during the delay.

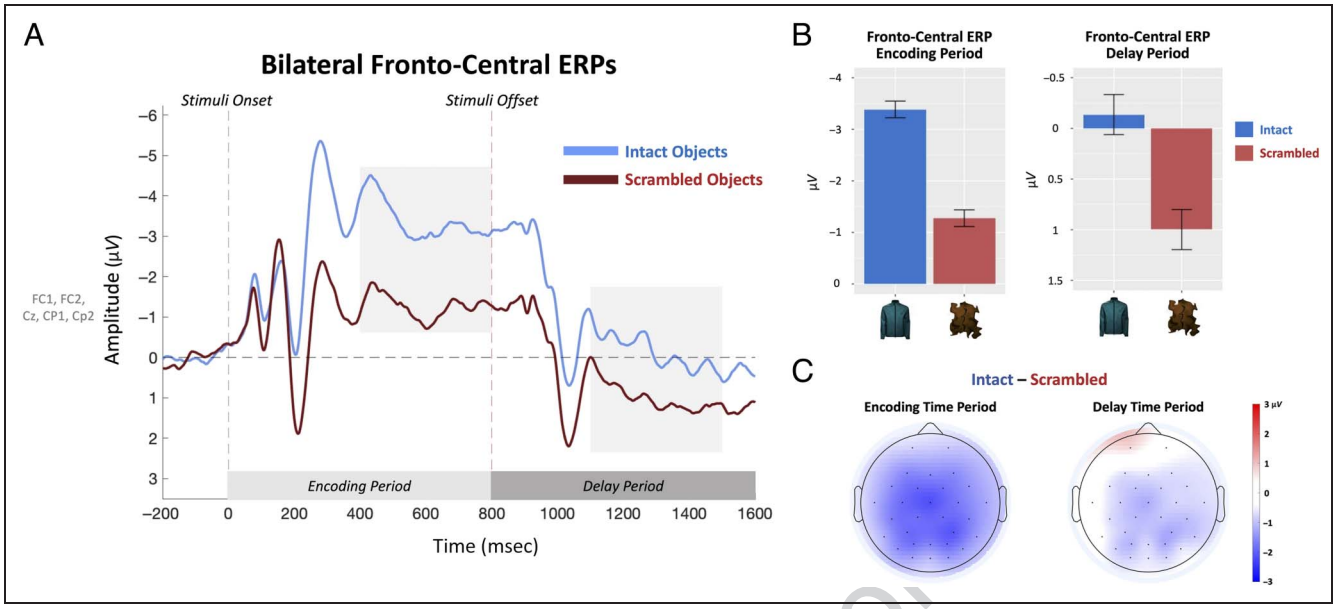

Figure 5. (A) Nonlateralized waveforms recorded over fronto-central electrode sites separately for intact and scrambled objects. Highlighted areas indicate the time windows for statistical analyses. (B) Mean ERP amplitudes during the encoding and delay time periods. (C) Spatial topographies of the intact-minus-scrambled object conditions for each time window.

DISCUSSION

We recently found improved working memory performance for colors when they were encoded as parts of meaningful objects, relative to colors that were superimposed on nonmeaningful shapes that were matched in visual complexity (Chung et al., 2023, 2024a; see also Loaiza et al., 2024). Here, we demonstrate that this performance benefit is accompanied by increased neural delay activity and earlier-arising neural stability for intact objects compared with scrambled objects. This finding of increased neural engagement contrasts with alternative theories, like efficient coding of color information (which would result in reduced memory engagement), or nonactive processes such as more effective retrieval at test from passive memory systems, like activated long-term memory (e.g., Cowan, 1988).

We also observed differences in the spatial topography across conditions: The CDA (independent of amplitude) appeared to be more spread out throughout parietal, central, and temporal sites in the intact object compared with the scrambled object condition that showed a more occipital focus. Such shifts in CDA topography may suggest the recruitment of additional neural populations in the intact object condition, possibly reflecting an electrophysiological correlate of the engagement of higher-level object or semantic regions (i.e., sensory recruitment; Adam et al., 2022; for similar shifts in CDA from working memory task relevance, see Breitinger et al., 2022). For example, it has been shown that colored objects (regardless of how diagnostic the colors are for a given object) activate both low-level perceptual regions and also higher-level visual regions that are tuned to objects and their associated colors (e.g., Lafer-Sousa et al., 2016; Bramão et al., 2010). Thus, simple features like colors may be coded—and maintained—redundantly across the visual hierarchy, creating stronger, more stable representations. Furthermore, associating simple features like color to real-world objects may activate additional semantic knowledge structures of these objects, effectively increasing memory dimensionality and thereby reducing interference (Wyble, Swan, & Callahan-Flintoft, 2016). This interpretation aligns with prior studies showing increased neural maintenance activity and improved performance when participants remember the identities of real-world objects rather than just colors (Thibeault et al., 2024; Asp et al., 2021; Brady et al., 2016). However, a key distinction is that these studies focused on working memory for entire object identities, whereas the present study specifically examined memory for colors alone. Importantly, the colors themselves were not semantically meaningful or diagnostic (e.g., a jacket could appear in any color). Thus, the current results significantly extend beyond previous work by demonstrating that increases in representational dimensionality due to links to semantic knowledge not only improve memory for the objects themselves but also provide an effective scaffold for actively maintaining their low-level and abstract visual features, even when those features are not directly related to the semantics of the object (Chung et al., 2023, 2024a). Overall, this suggests that expanded neural recruitment enables higher-dimensional working memory representations that support the maintenance of even simple features, either through redundant coding and/or by connecting lower-level visual features to semantic meaning in a hierarchically structured way.

Is it possible that the observed increase in CDA amplitude reflects memory for the intact objects' identities and not their colors? Previous studies have shown that some

aspects of object identity information can be incidentally present in working memory representations even when not explicitly task relevant (e.g., Chung et al., 2025; Sasin et al., 2023), suggesting that meaningful stimuli may support color working memory through such incidental associations. However, based on prior work, it seems rather unlikely that the CDA amplitude difference observed here solely reflects object-identity storage in the absence of color representation maintenance. Specifically, previous studies have demonstrated that the CDA amplitude primarily indexes active maintenance of task-relevant information and not task-irrelevant information, even when stimuli contain multiple features (e.g., remembering colors from color-orientation conjunctions; Woodman & Vogel, 2008). Other work has shown that incidental memories for stimulus features that are not probed at test are not robustly reflected in the CDA amplitude, even when those features are used for selection during the encoding phase (Zhu et al., 2022, Experiment 3). Similarly, Williams and Drew (2021) reported that processing of task-irrelevant real-world objects during a visual search was not reflected in the CDA (Williams & Drew, 2021, Experiment 1). Together, these studies strongly suggest that the CDA amplitude reflects storage of only task-relevant information—which in the present study is color. Therefore, based on this prior work, the current results are most compatible with the interpretation that the observed CDA increase reflects a boost in maintenance capacity for task-relevant color information and not solely incidental maintenance of object identities.

The present study used carefully generated control stimuli that matched the low-level visual features and complexity of real-world objects to ensure that observed neural differences cannot be attributed to differences in visual complexity. Especially, the task-relevant visual features (i.e., colors) were matched between the two conditions. This is particularly important as some previous studies have shown CDA amplitudes may be sensitive to large perceptual differences among stimuli (e.g., Rajsic et al., 2019; Woodman & Vogel, 2008), despite lateralized subtraction. Importantly, more complex but meaningless stimuli actually result in lower CDA amplitudes than simple stimuli, consistent with lower behavioral performance for such stimuli (Gao, Ding, Yang, Liang, & Shui, 2013; Gao, Li, Liang, Chen, Yin, & Shen, 2009); only stimuli that are both complex and meaningful result in higher CDA amplitudes compared with abstract stimuli, again consistent with higher behavioral performance for such stimuli (Thibeault et al., 2024; Asp et al., 2021; Brady et al., 2016). Overall, the findings showing differences in CDA amplitudes across different stimulus types even at same set sizes and with identical task-relevant features suggest that the CDA may reflect a broader neural marker of general memory strength in visual working memory (i.e., indexing how much task-relevant information is being held in visual working memory more generally; Merkel et al., 2021; Salahub et al., 2019; Gao et al., 2009) and is not just an assessment tool for discrete item limits (Balaban et al., 2019; Hakim et al., 2019; Fukuda et al., 2010; Ikkai et al., 2010).

Our multivariate pattern analysis across time revealed earlier stabilization of neural activity patterns in the real-world compared with the scrambled stimulus condition. This may reflect shifts in how working memory representations form over time. For instance, stable representation may emerge more rapidly for colors of meaningful objects due to readily available semantic structures that facilitate mapping the memoranda onto those higher-level structures. In contrast, color representations of meaningless objects may require longer time to reach stable neural activity patterns, resulting in greater pattern shifts. Although further work is needed to interpret this novel approach to analyzing lateralized ERPs in working memory (e.g., testing different set sizes or chunking effects), our findings open a new direction for EEG working memory research.

We found that the lateralized negativity (CDA) emerged earlier for real-world objects, with a large condition effect already present during the latter half of the encoding period, before the classic CDA window. This matches other recent studies that also reported lateralized ERP differences emerging during encoding when comparing working memory for meaningful versus nonmeaningful stimuli (Thibeault et al., 2024; Asp et al., 2021). This could reflect faster and more accurate encoding of the stimuli into working memory, as well as limits in how much information can be extracted and maintained during perception (Balaban & Luria, 2019; Tsubomi et al., 2013; for a review, see Emrich, Salahub, & Katus, 2022). Such early condition differences contrast with earlier claims in the literature of no effects of encoding time (Alvarez & Cavanagh, 2004; Luck & Vogel, 1997), but are consistent with newer work showing repeatedly that encoding format and time can play a critical role in working memory processes for simple stimuli (Quirk et al., 2020; Schurgin et al., 2020) and meaningful objects (Brady & Störmer, 2024; Chung et al., 2024a; Brady et al., 2016). The present data provide further support that memory capacity depends on limits that can be observed even when the stimuli are still on the screen and that real-world objects can provide a useful structure to initially build, and then maintain, robust representations.

Finally, our study also reveals a novel neural signature that appears to track processes related to recognizing intact versus scrambled objects. Beginning during encoding and continuing throughout the delay period, we observed a large nonlateralized slow-wave over frontocentral electrode sites that was more negative for intact than for scrambled objects. This suggests that differential processing of meaningful versus nonmeaningful stimuli emerges early during encoding and may in turn influence subsequent working memory processes. This sustained negativity resembles the well-known N400 component, typically associated with semantic processing of words in sentences (Kutas & Hillyard, 1980),[1] with more recent work showing sensitivity to visual-semantic knowledge

as well: The N400 amplitude has been shown to be more negative for less familiar or unrecognizable objects relative to recognizable ones (e.g., Enge et al., 2023; Rahman & Sommer, 2008) and for objects appearing in semantically incongruent (vs. congruent) scenes (e.g., toothbrush in kitchen; Võ & Wolfe, 2013). However, the polarity of the effect observed in our study was in the opposite direction, with unrecognizable scrambled objects eliciting a smaller negative deflection than recognizable objects. Interestingly, decreased negative deflections have been observed for "syntactically" incongruent objects in visual scenes (e.g., toothbrush in shower; Võ & Wolfe, 2013), as well as in the verbal domain, where scrambled letter strings evoked a smaller N400 amplitude compared with real words (Coch & Mitra, 2010; Bentin et al., 1999; Ziegler et al., 1997). Overall, this suggests that the N400 may be sensitive to multiple aspects of object and semantic understanding. Although further research is necessary to fully understand what cognitive processes underlie this component, our study demonstrates that its amplitude robustly distinguishes between intact versus scrambled objects, potentially extending previously observed ERP differences in the linguistic domain.[2]

In conclusion, our results show that working memory for simple features is shaped by the context these features are encoded in. Meaningful context at encoding—being part of a real-world object—promotes stronger neural engagement and earlier temporal stability of color memory representations during encoding and maintenance processes. Broadly, this indicates that active working memory processes, and consequently its capacity, are flexible, even with respect to a single feature dimension.

Acknowledgments

Special thanks to Sadye Law, our research assistant who helped with initial data collection and pilot experiments, and Alison Sasaki and Sam (Seho) Jung who helped finish data collection. We would like to acknowledge Thibeault and colleagues for making their data openly accessible, which enabled us to do a reanalysis of their EEG data in the Supplemental Materials.

Corresponding author: Yong Hoon Chung, Department of Psychological and Brain Sciences, Dartmouth College, Hanover, NH 03755, e-mail: yong.hoon.chung.gr@dartmouth.edu.

Data Availability Statement

All data and example analysis codes are available on the Open Science Framework (https://osf.io/bgmuw/). Supplemental Material can be accessed on this article's homepage: https://doi.org/10.1162/JOCN.a.2427.

Author Contributions

Yong Hoon Chung: Conceptualization; Data curation; Formal analysis; Investigation; Methodology; Project administration; Validation; Visualization; Writing—Original draft; Writing—Review & editing. Timothy Brady: Conceptualization; Formal analysis; Funding acquisition; Investigation; Methodology; Project administration; Resources; Supervision; Validation; Visualization; Writing—Review & editing. Viola Störmer: Conceptualization; Formal analysis; Funding acquisition; Investigation; Methodology; Project administration; Resources; Software; Supervision; Validation; Visualization; Writing—Original draft; Writing—review & editing.

Funding Information

T. F. B. is supported by the National Science Foundation grant 2141189.

Diversity in Citation Practices

Retrospective analysis of the citations in every article published in this journal from 2010 to 2021 reveals a persistent pattern of gender imbalance: Although the proportions of authorship teams (categorized by estimated gender identification of first author/last author) publishing in the *Journal of Cognitive Neuroscience* (*JoCN*) during this period were M(an)/M = .407, W(oman)/M = .32, M/W = .115, and W/W = .159, the comparable proportions for the articles that these authorship teams cited were M/M = .549, W/M = .257, M/W = .109, and W/W = .085 (Postle and Fulvio, *JoCN*, 34:1, pp. 1–3). Consequently, *JoCN* encourages all authors to consider gender balance explicitly when selecting which articles to cite and gives them the opportunity to report their article's gender citation balance.

Notes

1. Another similar well-known ERP is the FN400, a negative-going potential associated with familiarity recognition process, typically observed during episodic long-term memory tasks in which novel or less familiar items elicit more negative amplitudes (e.g., Stróżak et al., 2016). However, it is important to note that the current study involved a visual working memory task designed to limit the formation of long-term episodic traces for specific stimuli over time. Specifically, objects were rarely repeated, colors were randomly assigned, and participants had to maintain the colors of specific items on a given trial—memories of previous trials could support performance here.
2. A similar pattern of nonlateralized ERP result was observed in a previous study investigating visual working memory of identities of real-world objects and scrambled objects (Thibeault et al., 2024; see Supplemental Materials).

REFERENCES

Adam, K. C., Rademaker, R. L., & Serences, J. T. (2022). Evidence for, and challenges to, sensory recruitment models of visual working memory. *Visual memory* (pp. 5–25). Routledge. https://doi.org/10.4324/9781003158134-2

Adam, K. C. S., Robison, M. K., & Vogel, E. K. (2018). Contralateral delay activity tracks fluctuations in working memory performance. *Journal of Cognitive Neuroscience*,

30, 1229–1240. https://doi.org/10.1162/jocn_a_01233, PubMed: 29308988
Adam, K. C. S., Vogel, E. K., & Awh, E. (2017). Clear evidence for item limits in visual working memory. *Cognitive Psychology*, *97*, 79–97. https://doi.org/10.1016/j.cogpsych.2017.07.001, PubMed: 28734172
Alvarez, G. A., & Cavanagh, P. (2004). The capacity of visual short-term memory is set both by visual information load and by number of objects. *Psychological Science*, *15*, 106–111. https://doi.org/10.1111/j.0963-7214.2004.01502006.x, PubMed: 14738517
Asp, I. E., Störmer, V. S., & Brady, T. F. (2021). Greater visual working memory capacity for visually matched stimuli when they are perceived as meaningful. *Journal of Cognitive Neuroscience*, *33*, 902–918. https://doi.org/10.1162/jocn_a_01693, PubMed: 34449847
Awh, E., & Vogel, E. K. (2025). Working memory needs pointers. *Trends in Cognitive Sciences*, *29*, 230–241. https://doi.org/10.1016/j.tics.2024.12.006, PubMed: 39779443
Baddeley, A. D., & Hitch, G. J. (1974). Working memory. In G. H. Bower (Ed.), *Psychology of learning and motivation* (pp. 47–89). https://doi.org/10.1016/S0079-7421(08)60452-1
Balaban, H., Drew, T., & Luria, R. (2019). Neural evidence for an object-based pointer system underlying working memory. *Cortex*, *119*, 362–372. https://doi.org/10.1016/j.cortex.2019.05.008, PubMed: 31195317
Balaban, H., & Luria, R. (2019). Using the contralateral delay activity to study online processing of items still within view. In *Spatial learning and attention guidance* (pp. 107–128). Springer. https://doi.org/10.1007/7657_2019_22
Bays, P. M. (2014). Noise in neural populations accounts for errors in working memory. *Journal of Neuroscience*, *34*, 3632–3645. https://doi.org/10.1523/JNEUROSCI.3204-13.2014, PubMed: 24599462
Bays, P. M., Catalao, R. F. G., & Husain, M. (2009). The precision of visual working memory is set by allocation of a shared resource. *Journal of Vision*, *9*, 7.1–7.11. https://doi.org/10.1167/9.10.7, PubMed: 19810788
Bays, P. M., Schneegans, S., Ma, W. J., & Brady, T. F. (2024). Representation and computation in visual working memory. *Nature Human Behaviour*, *8*, 1016–1034. https://doi.org/10.1038/s41562-024-01871-2, PubMed: 38849647
Bentin, S., Mouchetant-Rostaing, Y., Giard, M. H., Echallier, J. F., & Pernier, J. (1999). ERP manifestations of processing printed words at different psycholinguistic levels: Time course and scalp distribution. *Journal of Cognitive Neuroscience*, *11*, 235–260. https://doi.org/10.1162/089892999563373, PubMed: 10402254
Brady, T. F., Konkle, T., Gill, J., Oliva, A., & Alvarez, G. A. (2013). Visual long-term memory has the same limit on fidelity as visual working memory. *Psychological Science*, *24*, 981–990. https://doi.org/10.1177/0956797612465439, PubMed: 23630219
Brady, T. F., & Störmer, V. S. (2022). The role of meaning in visual working memory: Real-world objects, but not simple features, benefit from deeper processing. *Journal of Experimental Psychology: Learning, Memory, and Cognition*, *48*, 942–958. https://doi.org/10.1037/xlm0001014, PubMed: 33764123
Brady, T. F., & Störmer, V. S. (2024). Comparing memory capacity across stimuli requires maximally dissimilar foils: Using deep convolutional neural networks to understand visual working memory capacity for real-world objects. *Memory & Cognition*, *52*, 595–609. https://doi.org/10.3758/s13421-023-01485-5, PubMed: 37973770
Brady, T. F., Störmer, V. S., & Alvarez, G. A. (2016). Working memory is not fixed-capacity: More active storage capacity for real-world objects than for simple stimuli. *Proceedings of the National Academy of Sciences, U.S.A.*, *113*, 7459–7464. https://doi.org/10.1073/pnas.1520027113, PubMed: 27325767
Bramão, I., Faísca, L., Forkstam, C., Reis, A., & Petersson, K. M. (2010). Cortical brain regions associated with color processing: An FMRI study. *Open Neuroimaging Journal*, *4*, 164–173. https://doi.org/10.2174/1874440001004010164, PubMed: 21270939
Breitinger, E., Pokorny, L., Biermann, L., Jarczok, T. A., Dundon, N. M., Roessner, V., et al. (2022). What makes somatosensory short-term memory maintenance effective? An EEG study comparing contralateral delay activity between sighted participants and participants who are blind. *Neuroimage*, *259*, 119407. https://doi.org/10.1016/j.neuroimage.2022.119407, PubMed: 35752414
Buschman, T. J., Siegel, M., Roy, J. E., & Miller, E. K. (2011). Neural substrates of cognitive capacity limitations. *Proceedings of the National Academy of Sciences, U.S.A.*, *108*, 11252–11255. https://doi.org/10.1073/pnas.1104666108, PubMed: 21690375
Carlisle, N. B., Arita, J. T., Pardo, D., & Woodman, G. F. (2011). Attentional templates in visual working memory. *Journal of Neuroscience*, *31*, 9315–9322. https://doi.org/10.1523/JNEUROSCI.1097-11.2011, PubMed: 21697381
Chung, Y. H., Brady, T. F., & Störmer, V. S. (2023). No fixed limit for storing simple visual features: Realistic objects provide an efficient scaffold for holding features in mind. *Psychological Science*, *34*, 784–793. https://doi.org/10.1177/09567976231171339, PubMed: 37227786
Chung, Y. H., Brady, T. F., & Störmer, V. S. (2024a). Sequential encoding aids working memory for meaningful objects' identities but not for their colors. *Memory & Cognition*, *52*, 2119–2131. https://doi.org/10.3758/s13421-023-01486-4, PubMed: 37948024
Chung, Y. H., Brady, T. F., & Störmer, V. S. (2024b). Meaningfulness and familiarity expand visual working memory capacity. *Current Directions in Psychological Science*, *33*, 275–282. https://doi.org/10.1177/09637214241262334
Chung, Y. H., Tam, J., Wyble, B., & Störmer, V. S. (2025). Conceptual information of meaningful objects is stored incidentally. *Journal of Experimental Psychology: Learning, Memory, and Cognition*, *51*, 82–96. https://doi.org/10.1037/xlm0001339, PubMed: 38573722
Clark, J. H. (1924). The Ishihara test for color blindness. *American Journal of Physiological Optics*, *5*, 269–276.
Coch, D., & Mitra, P. (2010). Word and pseudoword superiority effects reflected in the ERP waveform. *Brain Research*, *1329*, 159–174. https://doi.org/10.1016/j.brainres.2010.02.084, PubMed: 20211607
Cowan, N. (1988). Evolving conceptions of memory storage, selective attention, and their mutual constraints within the human information-processing system. *Psychological Bulletin*, *104*, 163–191. https://doi.org/10.1037/0033-2909.104.2.163, PubMed: 3054993
Cowan, N. (2001). The magical number 4 in short-term memory: A reconsideration of mental storage capacity. *Behavioral and Brain Sciences*, *24*, 87–114. https://doi.org/10.1017/S0140525X01003922, PubMed: 11515286
Delorme, A., & Makeig, S. (2004). EEGLAB: An open source toolbox for analysis of single-trial EEG dynamics including independent component analysis. *Journal of Neuroscience Methods*, *134*, 9–21. https://doi.org/10.1016/j.jneumeth.2003.10.009, PubMed: 15102499
Emrich, S. M., Salahub, C., & Katus, T. (2022). Sensory delay activity: More than an electrophysiological index of working memory load. *Journal of Cognitive Neuroscience*, *35*, 135–148. https://doi.org/10.1162/jocn_a_01922, PubMed: 36223227

Enge, A., Süß, F., & Rahman, R. A. (2023). Instant effects of semantic information on visual perception. *Journal of Neuroscience*, *43*, 4896–4906. https://doi.org/10.1523/JNEUROSCI.2038-22.2023, PubMed: 37286353

Fukuda, K., Awh, E., & Vogel, E. K. (2010). Discrete capacity limits in visual working memory. *Current Opinion in Neurobiology*, *20*, 177–182. https://doi.org/10.1016/j.conb.2010.03.005, PubMed: 20362427

Gao, Z., Ding, X., Yang, T., Liang, J., & Shui, R. (2013). Coarse-to-fine construction for high-resolution representation in visual working memory. *PloS One*, *8*, e57913. https://doi.org/10.1371/journal.pone.0057913, PubMed: 23469103

Gao, Z., Li, J., Liang, J., Chen, H., Yin, J., & Shen, M. (2009). Storing fine detailed information in visual working memory—Evidence from event-related potentials. *Journal of Vision*, *9*, 17. https://doi.org/10.1167/9.7.17, PubMed: 19761332

Hakim, N., Adam, K. C. S., Gunseli, E., Awh, E., & Vogel, E. K. (2019). Dissecting the neural focus of attention reveals distinct processes for spatial attention and object-based storage in visual working memory. *Psychological Science*, *30*, 526–540. https://doi.org/10.1177/0956797619830384, PubMed: 30817220

Hillyard, S. A., & Galambos, R. (1970). Eye movement artifact in the CNV. *Electroencephalography and Clinical Neurophysiology*, *28*, 173–182. https://doi.org/10.1016/0013-4694(70)90185-9, PubMed: 4189528

Ikkai, A., McCollough, A. W., & Vogel, E. K. (2010). Contralateral delay activity provides a neural measure of the number of representations in visual working memory. *Journal of Neurophysiology*, *103*, 1963–1968. https://doi.org/10.1152/jn.00978.2009, PubMed: 20147415

Kutas, M., & Hillyard, S. A. (1980). Reading senseless sentences: Brain potentials reflect semantic incongruity. *Science*, *207*, 203–205. https://doi.org/10.1126/science.7350657, PubMed: 7350657

Lafer-Sousa, R., Conway, B. R., & Kanwisher, N. G. (2016). Color-biased regions of the ventral visual pathway lie between face- and place-selective regions in humans, as in macaques. *Journal of Neuroscience*, *36*, 1682–1697. https://doi.org/10.1523/JNEUROSCI.3164-15.2016, PubMed: 26843649

Liu, J., Zhang, H., Yu, T., Ni, D., Ren, L., Yang, Q., et al. (2020). Stable maintenance of multiple representational formats in human visual short-term memory. *Proceedings of the National Academy of Sciences, U.S.A.*, *117*, 32329–32339. https://doi.org/10.1073/pnas.2006752117, PubMed: 33288707

Loaiza, V. M., Cheung, H. W., & Goldenhaus-Manning, D. T. (2024). What you don't know can't hurt you: Retro-cues benefit working memory regardless of prior knowledge in long-term memory. *Psychonomic Bulletin & Review*, *31*, 1–12. https://doi.org/10.3758/s13423-023-02408-w, PubMed: 37932579

Lopez-Calderon, J., & Luck, S. J. (2014). ERPLAB: An open-source toolbox for the analysis of event-related potentials. *Frontiers in Human Neuroscience*, *8*, 213. https://doi.org/10.3389/fnhum.2014.00213, PubMed: 24782741

Luck, S. J. (2014). *An introduction to the event-related potential technique*. MIT Press.

Luck, S. J., & Vogel, E. K. (1997). The capacity of visual working memory for features and conjunctions. *Nature*, *390*, 279–281. https://doi.org/10.1038/36846, PubMed: 9384378

Luck, S. J., & Vogel, E. K. (2013). Visual working memory capacity: From psychophysics and neurobiology to individual differences. *Trends in Cognitive Sciences*, *17*, 391–400. https://doi.org/10.1016/j.tics.2013.06.006, PubMed: 23850263

Luria, R., Balaban, H., Awh, E., & Vogel, E. K. (2016). The contralateral delay activity as a neural measure of visual working memory. *Neuroscience & Biobehavioral Reviews*, *62*, 100–108. https://doi.org/10.1016/j.neubiorev.2016.01.003, PubMed: 26802451

McCarthy, G., & Wood, C. C. (1985). Scalp distributions of event-related potentials: An ambiguity associated with analysis of variance models. *Electroencephalography and Clinical Neurophysiology*, *62*, 203–208. https://doi.org/10.1016/0168-5597(85)90015-2, PubMed: 2581760

McCollough, A. W., Machizawa, M. G., & Vogel, E. K. (2007). Electrophysiological measures of maintaining representations in visual working memory. *Cortex*, *43*, 77–94. https://doi.org/10.1016/S0010-9452(08)70447-7, PubMed: 17334209

Merkel, C., Bartsch, M. V., Schoenfeld, M. A., Vellage, A.-K., Müller, N. G., & Hopf, J.-M. (2021). A direct neural measure of variable precision representations in visual working memory. *Journal of Neurophysiology*, *126*, 1430–1439. https://doi.org/10.1152/jn.00230.2021, PubMed: 34550022

Predovan, D., Prime, D., Arguin, M., Gosselin, F., Dell'Acqua, R., & Jolicœur, P. (2009). On the representation of words and nonwords in visual short-term memory: Evidence from human electrophysiology. *Psychophysiology*, *46*, 191–199. https://doi.org/10.1111/j.1469-8986.2008.00753.x, PubMed: 19055498

Quirk, C., Adam, K. C. S., & Vogel, E. K. (2020). No evidence for an object working memory capacity benefit with extended viewing time. *eNeuro*, *7*, ENEURO.0150-20.2020. https://doi.org/10.1523/ENEURO.0150-20.2020, PubMed: 32859722

Rahman, R. A., & Sommer, W. (2008). Seeing what we know and understand: How knowledge shapes perception. *Psychonomic Bulletin & Review*, *15*, 1055–1063. https://doi.org/10.3758/PBR.15.6.1055, PubMed: 19001567

Rajsic, J., Burton, J. A., & Woodman, G. F. (2019). Contralateral delay activity tracks the storage of visually presented letters and words. *Psychophysiology*, *56*, e13282. https://doi.org/10.1111/psyp.13282, PubMed: 30246442

Roy, Y., & Faubert, J. (2023). Is the contralateral delay activity (CDA) a robust neural correlate for visual working memory (VWM) tasks? A reproducibility study. *Psychophysiology*, *60*, e14180. https://doi.org/10.1111/psyp.14180, PubMed: 36124370

Salahub, C., Lockhart, H. A., Dube, B., Al-Aidroos, N., & Emrich, S. M. (2019). Electrophysiological correlates of the flexible allocation of visual working memory resources. *Scientific Reports*, *9*, 19428. https://doi.org/10.1038/s41598-019-55948-4, PubMed: 31857657

Sasin, E., Markov, Y., & Fougnie, D. (2023). Meaningful objects avoid attribute amnesia due to incidental long-term memories. *Scientific Reports*, *13*, 14464. https://doi.org/10.1038/s41598-023-41642-z, PubMed: 37660090

Sassenhagen, J., & Draschkow, D. (2019). Cluster-based permutation tests of MEG/EEG data do not establish significance of effect latency or location. *Psychophysiology*, *56*, e13335. https://doi.org/10.1111/psyp.13335, PubMed: 30657176

Schurgin, M. W., Wixted, J. T., & Brady, T. F. (2020). Psychophysical scaling reveals a unified theory of visual memory strength. *Nature Human Behaviour*, *4*, 1156–1172. https://doi.org/10.1038/s41562-020-00938-0, PubMed: 32895546

Shin, H., & Ma, W. J. (2017). Visual short-term memory for oriented, colored objects. *Journal of Vision*, *17*, 12. https://doi.org/10.1167/17.9.12, PubMed: 28813568

Stojanoski, B., & Cusack, R. (2014). Time to wave good-bye to phase scrambling: Creating controlled scrambled images

using diffeomorphic transformations. *Journal of Vision*, *14*, 6. https://doi.org/10.1167/14.12.6, PubMed: 25301014
Stróżak, P., Abedzadeh, D., & Curran, T. (2016). Separating the FN400 and N400 potentials across recognition memory experiments. *Brain Research*, *1635*, 41–60. https://doi.org/10.1016/j.brainres.2016.01.015, PubMed: 26776478
Spaak, E., Watanabe, K., Funahashi, S., & Stokes, M. G. (2017). Stable and dynamic coding for working memory in primate prefrontal cortex. *Journal of Neuroscience*, *37*, 6503–6516. https://doi.org/10.1523/JNEUROSCI.3364-16.2017, PubMed: 28559375
Thibeault, A. M. L., Stojanoski, B., & Emrich, S. M. (2024). Investigating the effects of perceptual complexity versus conceptual meaning on the object benefit in visual working memory. *Cognitive, Affective, & Behavioral Neuroscience*, *24*, 453–468. https://doi.org/10.3758/s13415-024-01158-z, PubMed: 38291307
Torres, R. E., Duprey, M. S., Campbell, K. L., & Emrich, S. M. (2025). Not all objects are created equal: The object benefit in visual working memory is supported by greater recollection-like memory, but only for memorable objects. *Memory & Cognition*, *53*, 1343–1355. https://doi.org/10.3758/s13421-024-01655-z, PubMed: 39467965
Tsubomi, H., Fukuda, K., Watanabe, K., & Vogel, E. K. (2013). Neural limits to representing objects still within view. *Journal of Neuroscience*, *33*, 8257–8263. https://doi.org/10.1523/JNEUROSCI.5348-12.2013, PubMed: 23658165
Unsworth, N., Fukuda, K., Awh, E., & Vogel, E. K. (2015). Working memory delay activity predicts individual differences in cognitive abilities. *Journal of Cognitive Neuroscience*, *27*, 853–865. https://doi.org/10.1162/jocn_a_00765, PubMed: 25436671
Vogel, E. K., & Machizawa, M. G. (2004). Neural activity predicts individual differences in visual working memory capacity. *Nature*, *428*, 748–751. https://doi.org/10.1038/nature02447, PubMed: 15085132
Vogel, E. K., McCollough, A. W., & Machizawa, M. G. (2005). Neural measures reveal individual differences in controlling access to working memory. *Nature*, *438*, 500–503. https://doi.org/10.1038/nature04171, PubMed: 16306992
Võ, M. L.-H., & Wolfe, J. M. (2013). Differential electrophysiological signatures of semantic and syntactic scene processing. *Psychological Science*, *24*, 1816–1823. https://doi.org/10.1177/0956797613476955, PubMed: 23842954
Williams, L. H., & Drew, T. (2021). Maintaining rejected distractors in working memory during visual search depends on search stimuli: Evidence from contralateral delay activity. *Attention, Perception, & Psychophysics*, *83*, 67–84. https://doi.org/10.3758/s13414-020-02127-7, PubMed: 33000442
Woodman, G. F., & Vogel, E. K. (2008). Selective storage and maintenance of an object's features in visual working memory. *Psychonomic Bulletin & Review*, *15*, 223–229. https://doi.org/10.3758/PBR.15.1.223, PubMed: 18605507
Wyble, B., Swan, G., & Callahan-Flintoft, C. (2016). Measuring visual memory in its native format. *Trends in Cognitive Sciences*, *20*, 790–791. https://doi.org/10.1016/j.tics.2016.08.012, PubMed: 27623428
Zhu, P., Fu, Y., Wyble, B., Shen, M., & Chen, H. (2022). A new aspect of cognitive selectivity: Working memory reselection for attended information. *PsyArXiv*. https://doi.org/10.31234/osf.io/fzwp3
Ziegler, J. C., Besson, M., Jacobs, A. M., Nazir, T. A., & Carr, T. H. (1997). Word, pseudoword, and nonword processing: A multitask comparison using event-related brain potentials. *Journal of Cognitive Neuroscience*, *9*, 758–775. https://doi.org/10.1162/jocn.1997.9.6.758, PubMed: 23964598